

PLANNING WITH UNCERTAINTY: DEEP EXPLORATION IN MODEL-BASED REINFORCEMENT LEARNING

Yaniv Oren, Matthijs T. J. Spaan & Wendelin Böhmer

Department of Computer Science

Delft University of Technology

Mekelweg 5, 2628 CD Delft, the Netherlands

{y.oren,m.t.j.spaan,j.w.bohmer}@tudelft.nl

ABSTRACT

Deep model-based Reinforcement Learning (RL) has shown super-human performance in many challenging domains. Low sample efficiency and limited exploration remain as leading obstacles in the field, however. In this paper, we demonstrate deep exploration in model-based RL by incorporating epistemic uncertainty into planning trees, circumventing the standard approach of propagating uncertainty through value learning. We evaluate this approach with the state of the art model-based RL algorithm MuZero, and extend its training process to stabilize learning from explicitly-exploratory trajectories. In our experiments planning with uncertainty is able to demonstrate effective deep exploration with standard uncertainty estimation mechanisms, and with it significant gains in sample efficiency.

1 INTRODUCTION

In February 2022, state of the art performance in video compression on YouTube videos has been achieved with the algorithm MuZero (Mandhane et al., 2022; Schrittwieser et al., 2020), setting a new milestone in successful deployments of reinforcement learning (RL). MuZero is a deep model-based RL algorithm that learns an abstracted model of the environment through interactions, and uses it for planning. While able to achieve state of the art performance in extremely challenging domains, MuZero is limited by on-policy exploration that relies on random action selection. Effective, informed exploration is crucial in many problem settings (O’Donoghue et al., 2018), and can induce up to exponential gain in sample efficiency (Osband et al., 2016).

Standard approaches for exploration rely on estimates of *epistemic uncertainty* (uncertainty that is caused by a lack of information, Hüllermeier & Waegeman, 2021) to drive exploration into under-explored areas of the state-action space (Bellemare et al., 2016; Sekar et al., 2020) or the learner’s parameter space (Russo et al., 2018). These approaches often incorporate the uncertainty into value-learning as a non-stationary reward bonus (Oudeyer & Kaplan, 2009) or to directly approximate the total uncertainty in a value-like prediction propagated over future actions (O’Donoghue et al., 2018) to achieve exploration that is *deep*. We refer to deep exploration as exploration that is able to propagate uncertainty from distant areas of the state-action space into local decisions and is consistent over multiple time-steps. This type of exploration enables the agent to aim for and reach these interesting areas from its initial or current state.

While propagating the uncertainty from future actions through the value function enables propagation over a far horizon, it also introduces several problems. First, the values become non-stationary with the uncertainty bonus, introducing potential instability into the value learning. Second, the horizon of the propagation is limited in the number of training steps: uncertainty in states that are far from the initial state will only propagate to the initial state after sufficiently many training steps, and not immediately. Third, the propagation speed is directly correlated with number of training steps, and as a result uncertainty from encountered high-uncertainty areas of the state space that are not trained often will not (or barely) propagate. To overcome these problems, this paper proposes to propagate uncertainty through the planning-tree of model-based RL instead of a neural-network value function. This facilitates the decoupling of the propagation from the learning process by

propagating the uncertainty during online inference, and addresses the challenges originating from propagating the uncertainty through value learning. To demonstrate that propagating uncertainty in the online planning-trees of model-based methods like MuZero can provide deep exploration, this paper’s contribution is divided into three parts. First, we propose a framework for propagating epistemic uncertainty about the planning process itself through a planning tree, for example, in Monte Carlo Tree Search (MCTS, see Browne et al., 2012, for an overview) with learned models. Second, we propose to harness planning with uncertainty to achieve deep exploration in the standard RL setting (in difference to prior approaches, Sekar et al., 2020, that required a pre-training phase to explore), by modifying the objective of an online planning phase with epistemic uncertainty, which we dub online planning to explore, or OP2E. Third, to stabilize learning from off-policy exploratory decisions in MuZero, we extend MuZero’s training process by splitting training into exploration episodes and exploitation episodes, and generating the value and policy targets differently depending on the type of episode. We conduct experiments against hard-exploration tasks to evaluate the capacity of OP2E to achieve deep exploration. In addition, we conduct an ablation study to evaluate the individual effects of the different extensions we propose to training from explicitly exploratory trajectories. In our experiments OP2E was able to significantly outperform vanilla MuZero in hard-exploration tasks, demonstrating effective deep exploration resulting in significant gains in sample efficiency. Our ablation study points out the potential value of discerning between positive and negative exploration trajectories and generating policy targets accordingly, as well as the resilience of n-step value targets to the presence of strongly off-policy trajectories.

This paper is organized as follows: Section 2 provides relevant background for model-based RL, MuZero and epistemic uncertainty estimation in deep learning. Section 3 describes our contributions, starting with the framework for uncertainty propagation, followed by our approach for modifying planning with uncertainty to achieve deep exploration (OP2E) and finally the extensions proposed to stabilize learning from exploratory decisions. Section 4 evaluates OP2E against two hard-exploration tasks in comparison with vanilla MuZero and presents an ablation study of the different extensions to learning from exploratory decisions. Section 5 discusses related work, and Section 6 concludes the paper and discusses future work.

2 BACKGROUND

2.1 REINFORCEMENT LEARNING

In reinforcement learning (RL), an agent learns a behavior policy through interactions with an environment, by observing states (or observations), executing actions and receiving rewards. The environment is represented with a Markov Decision Process (MDP, Bellman, 1957), or a partially-observable MDP (POMDP, Åström, 1965). An MDP M is a tuple: $\mathcal{M} = \langle S, A, \rho, P, R \rangle$, where S is a set of states, A a set of actions, ρ a probability distribution over the state space specifying the probability of starting at each state $s \in S$, $R : S \times A \rightarrow \mathbb{R}$ a bounded reward function, and $P : S \times A \times S \rightarrow [0, 1]$ is a transition function, where $P(s'|s, a)$ specifies the probability of transitioning from state s to state s' after executing action a . A POMDP \mathcal{M}' is a tuple $\langle S, A, \rho, P, R, \Omega, O \rangle$ as well. When interacting with a POMDP, an agent does not observe the state of the system directly. Instead, it observes observations $o \in \Omega$. The function $O : S \times A \times \Omega \rightarrow [0, 1]$ specifies the probability $O(o|s, a)$ of observing a possible observation o at each transition. The agent’s behavior is described by a policy $\pi(a|s)$, a conditional distribution that describes for every state s the probability of choosing action a . The RL agent usually aims for a policy that maximizes the *expected cumulative discounted reward over time* (expected return).

In model based reinforcement learning (MBRL) the agent learns a model of the environment through interactions, and uses it to optimize its policy, often through *planning*. In deep MBRL (DMBRL) the agent utilizes deep neural networks (DNNs) as function approximators. Many RL approaches rely on learning a state-action *Q-value function* $Q^\pi(s, a) = R(s, a) + \gamma \mathbb{E}[V^\pi(s')|s' \sim P(\cdot|s, a)]$ or the corresponding state *value function* $V^\pi(s) = \mathbb{E}[Q^\pi(s, a)|a \sim \pi(\cdot|s)]$, which represents the expected return from starting in state s (and possibly action a) and then following policy π .

2.2 MONTE CARLO TREE SEARCH

MCTS is a planning algorithm that constructs a planning tree with the current state s_t at its root, to estimate the objective, here $\max_{\pi} Q^{\pi}(s_t, a)$ for every available action $a \in A$. The algorithm repeatedly performs the following four steps: *trajectory selection, expansion, simulation and backup*. Starting from the root node $n_0 \equiv s_t$, the algorithm selects a trajectory in the existing tree based on the averaged returns $q(n_k, a)$ experienced in past trajectories selecting the action a in the same node n_k , and one of many search heuristics, such as an Upper Confidence Bound for Trees (UCT, Kocsis & Szepesvári, 2006):

$$a_k = \arg \max_{a \in A} q(n_k, a) + 2C_p \sqrt{\frac{2 \log(\sum_{a'} N(n_k, a'))}{N(n_k, a)}} \quad (1)$$

where $N(n_k, a)$ denotes how many times action a has been executed in node n_k . The trajectory selection proceeds iteratively until it arrives at a leaf node, that has yet to be expanded in the tree. MCTS expands the node and estimates its initial value with a rollout from a random policy. However, Alpha Go/Zero (Silver et al., 2016; 2017; 2018) uses a value function $v(n_k)$ that is approximated by a neural network to estimate the leaf’s value and chooses potential actions a to expand first with another approximation of the MCTS policy $\pi(a|n_k)$. Last, MCTS propagates the return (discounted reward for visited nodes plus leaf’s value) back along the planning trajectory, updating the averaged returns $q(n_k, a_k)$, all the way up to the root of the tree. By choosing different trajectory selection heuristics, MCTS can be used to optimize for different objectives. At the root of the tree, the value $V^{\pi}(s_t)$ of current state s_t is estimated based on the averaged returns experienced through every action a , and averaged over the actions:

$$V^{\pi}(s_t) \approx \sum_{a \in A} \frac{q(n_0, a) N(n_0, a)}{\sum_{a' \in A} N(n_0, a')} =: v_t^{\pi} \quad (2)$$

2.3 MUZERO

MuZero is a MBRL algorithm that learns an abstracted model of the environment from interactions, and uses it for planning with MCTS. The model learned by MuZero consists of 5 functions that are approximated with neural networks: the representation function $\hat{s}_0 = g(o_t)$, the transition function $\hat{s}_{k+1} = f(\hat{s}_k, a_k)$, the expected-reward function $\hat{r}_k = r(\hat{s}_k, a_k)$, the value function $\hat{v}_k = v(\hat{s}_k)$ and policy function $p(\hat{s}_k) = \pi(a|\hat{s}_k)$. In practice, the representation and dynamics are only used as node-representations $\hat{s}_k = n_k$ in the MCTS planning tree, and only need to represent the states of the environment as far as they are useful for the MCTS. The variation of MCTS used by MuZero approximates the value of a leaf-node in the expansion step with a direct predictions from the value function v instead of Monte-Carlo simulations. MCTS is used in MuZero for two purposes: first, for inference of the best action to execute in the environment, and second to generate targets for the policy and value functions. MuZero is trained with on-policy value and policy targets. The policy targets are the relative visitations numbers to each child of the root node, and the value targets are n -step TD targets:

$$v_t^{target} = \sum_{i=0}^{n-1} \gamma^i r_{t+i}^{\pi} + \gamma^n v_{t+n}^{\pi},$$

Where π is the policy that was executed in the environment which was induced by the MCTS at every time step. With the Reanalyse variation of MuZero (Schrittwieser et al., 2021), the policy and value targets are constantly updated in the replay buffer based on new planning trees that are computed by Reanalyse, turning MuZero Reanalyse into a (mostly) off-policy algorithm. The updated value targets are still n -step targets that use the sum of rewards $\sum_{i=0}^{n-1} \gamma^i r_{t+i}^{\pi}$ observed in the environment following policy π . This prevents MuZero Reanalyse from being a completely off-policy algorithm and makes it challenging to learn from explicitly-exploratory trajectories that do not follow the current exploitation policy.

2.4 EPISTEMIC UNCERTAINTY ESTIMATION IN DEEP LEARNING

Defining, quantifying and estimating predictive epistemic uncertainty is an active field of machine learning research that encompasses many approaches and many methods (Hüllermeier & Waegeman, 2021; Jain et al., 2021). In this work we assume epistemic uncertainty can be represented with

probability theory, and estimated as the variance in a probability distribution of predictions that are consistent with the observations $\text{Var}(X|o_t) = \mathbb{V}_X[X|o_t]$, which is a standard approach for epistemic uncertainty quantification. This allows us to investigate the propagation of uncertainty in predictions of a node n_k in a planning tree with respect to observations and a trajectory of actions through the lens of variance propagation $\mathbb{V}_{X_k}[X_k|o_t, a_{0:k}]$ which is well studied.

To directly estimate the epistemic variance in the local predictions of value and reward used by MuZero in planning we use two methods: deep ensembles with prior functions (Osband et al., 2018) and state-visitation counting. Ensembles are scalable to arbitrarily large state spaces as well as computationally inexpensive for small ensemble sizes. The epistemic uncertainty estimation ensembles provide however is not necessarily reliable. As an additional method that is able to provide reliable estimates of epistemic uncertainty we use state visitation counting. This method estimates epistemic uncertainty directly based on the number of times each state or state-action pair has been visited. While a toy method, visitations counting enables us to evaluate the approach in the presence of both reliable and unreliable uncertainty estimators. Additional details regarding applying these methods to the functions used by MuZero can be found in appendix B.

3 CONTRIBUTIONS

Our approach modifies MCTS to plan for an exploratory objective rather than an exploitative objective, i.e., to predict the best action that can be taken in the environment for gathering relevant information rather than for highest expected return. To apply this approach with MuZero as a use-case, we take three steps. First, we propose approximations for uncertainty propagated through a planning tree, forward and back (Section 3.1). Second, we propose to modify the UCT operator with the propagated uncertainty to optimize action selection for exploration with a so-called optimistic objective (Section 3.2). Third, we propose to extend the training process of MuZero by introducing a distinction between exploration and exploitation episodes and by modifying the target generation from exploratory trajectories. The target generation is extended to discern between exploration trajectories that resulted in returns that are higher than the agent’s value approximations for the same initial state, and trajectories that did not. For exploration trajectories that resulted in improved returns, the exploratory decisions become the targets from the learning trajectory. Otherwise, the agent’s exploitative approximations provide the target (Section 3.3).

3.1 PROPAGATING UNCERTAINTY IN A PLANNING TREE

Selecting a path $n_{0:T}$ through a decision tree is equivalent to choosing a sequence of T actions $a_{0:T-1}$ that end up in a leaf node n_T . In standard MCTS a deterministic model predicts the encountered rewards r_k in nodes $n_k, 0 \leq k < T$, and the estimated value v_T at the leaf n_T . These are used to update the n -step discounted return ν_k of each node n_k on the selected path:

$$\nu_k := \sum_{i=k}^{T-1} \gamma^{i-k} r_i + \gamma^T v_T = r_k + \gamma \nu_{k+1}, \quad 0 \leq k < T, \quad \nu_T = v_T \quad (3)$$

If the model that produced states, rewards and values cannot be fully trusted, r_k and v_T can be formulated as random variables in a Markov chain that is connected by random state-variables $s_k, 0 \leq k \leq T$. These correspond to the nodes on the path, the corresponding states, or their representations, but not necessarily to the output \hat{s}_k of any MuZero transition model (Section 2.3).

In exploration, paths that lead to under-explored states, or states where the model is not reliable yet, should be incentivized. In line with optimistic exploration literature, we incentivize choosing actions in the environment associated with paths in the planning tree that have *uncertain* returns ν_0 in order to both improve the model as well as find high-reward interactions. For this we need to estimate the variance $\mathbb{V}_\nu[\nu_0|o_t, a_{0:T-1}]$ of the return along a selected path $a_{0:T-1}$, starting with observation o_t . To improve readability, we will omit in the following the condition on actions and observation, for example, $\mathbb{V}_\nu(\nu_0) \equiv \mathbb{V}_\nu[\nu_0|o_t, a_{0:T-1}]$.

We will begin by deriving the mean and variance of the distribution of state-variables in the Markov chain for a given sequence of actions $a_{0:T-1}$. Let us assume we are given a differentiable transition function $f(s_k, a_k) := \mathbb{E}_{s_{k+1}}[s_{k+1}|s_k, a_k] \in \mathbb{R}^{|S|}$, which predicts the average next state, and a differentiable uncertainty function $\Sigma(s_k, a_k) := \mathbb{V}_{s_{k+1}}[s_{k+1}|s_k, a_k] \in \mathbb{R}^{|S| \times |S|}$ that yields the

covariance matrix of the distribution. We will use an epistemic uncertainty measure to compute the latter, but in principle these functions could represent any distribution, containing any kind of uncertainty, epistemic or otherwise. We assume that the mean \bar{s}_0 of the first state-variable s_0 is given as an encoding function $\bar{s}_0 = \mathbb{E}_{s_0}[s_0|o_t] = g(o_t)$, like in MuZero. The mean \bar{s}_{k+1} of a later state-variable s_{k+1} can be approximated with a 1st order Taylor expansion around the previous mean $\bar{s}_k := \mathbb{E}_{s_k}[s_k]$:

$$\begin{aligned}\bar{s}_{k+1} &:= \mathbb{E}_{s_{k+1}}[s_{k+1}] = \mathbb{E}_{s_k}[\mathbb{E}_{s_{k+1}}[s_{k+1}|s_k, a_k]] = \mathbb{E}_{s_k}[f(s_k, a_k)] \\ &\approx \mathbb{E}_{s_k}[f(\bar{s}_k, a_k) + (s_k - \bar{s}_k)^\top \nabla_s f(s, a_k)|_{s=\bar{s}_k}] = f(\bar{s}_k, a_k).\end{aligned}\quad (4)$$

To approximate the covariance $\bar{\Sigma}_{k+1} := \mathbb{V}_{s_{k+1}}[s_{k+1}]$, we need the *law of total variance* where for two random variables x and y holds $\mathbb{V}_y[y] = \mathbb{E}_x[\mathbb{V}_y[y|x]] + \mathbb{V}_x[\mathbb{E}_y[y|x]]$ (see appendix A for a proof in our notation), and again a 1st order Taylor approximation around the previous mean state \bar{s}_k :

$$\begin{aligned}\bar{\Sigma}_{k+1} &:= \mathbb{V}_{s_{k+1}}[s_{k+1}] = \underbrace{\mathbb{E}_{s_k}[\mathbb{V}_{s_{k+1}}[s_{k+1}|s_k]]}_{\Sigma(\bar{s}_k, a_k)} + \underbrace{\mathbb{V}_{s_k}[\mathbb{E}_{s_{k+1}}[s_{k+1}|s_k]]}_{\mathbf{J}_f(\bar{s}_k, a_k) \bar{\Sigma}_k \mathbf{J}_f(\bar{s}_k, a_k)^\top} \\ &\approx \Sigma(\bar{s}_k, a_k) + \mathbf{J}_f(\bar{s}_k, a_k) \bar{\Sigma}_k \mathbf{J}_f(\bar{s}_k, a_k)^\top.\end{aligned}\quad (5)$$

Note that here $f(s_k, a_k) - \mathbb{E}_{s_k}[f(s_k, a_k)] \approx (s_k - \bar{s}_k)^\top \nabla_s f(s, a_k)|_{s=\bar{s}_k} =: (s_k - \bar{s}_k)^\top \mathbf{J}_f(\bar{s}_k, a_k)^\top$, where $\mathbf{J}_f(\bar{s}_k, a_k)$ denotes the Jacobian matrix of function f at state \bar{s}_k and action a_k . Using these state statistics, we can derive the means and variances of causally connected variables like rewards and values. We assume that the conditional reward distribution has mean $r(s_k, a_k) := \mathbb{E}_{r_k}[r_k|s_k, a_k]$ and variance $\sigma_r^2(s_k, a_k) := \mathbb{V}_{r_k}[r_k|s_k, a_k]$, and that the conditional value distribution has mean $v(s_T) := \mathbb{E}_{v_T}[v_T|s_T]$ and variance $\sigma_v^2(s_T) := \mathbb{V}_{v_T}[v_T|s_T]$. Analogous to above we can derive:

$$\bar{r}_k := \mathbb{E}_{r_k}[r_k] \approx r(\bar{s}_k, a_k), \quad \mathbb{V}_{r_k}[r_k] \approx \sigma_r^2(\bar{s}_k, a_k) + \mathbf{J}_r(\bar{s}_k, a_k) \bar{\Sigma}_k \mathbf{J}_r(\bar{s}_k, a_k)^\top, \quad (6)$$

$$\bar{v}_T := \mathbb{E}_{v_T}[v_T] \approx v(\bar{s}_T), \quad \mathbb{V}_{v_T}[v_T] \approx \sigma_v^2(\bar{s}_T) + \mathbf{J}_v(\bar{s}_k) \bar{\Sigma}_k \mathbf{J}_v(\bar{s}_k)^\top. \quad (7)$$

If we assume that r_k and the n -step return ν_{k+1} from Equation 3 are independent, we can compute

$$\mathbb{E}_{\nu_k}[\nu_k] = \mathbb{E}_{r_k \nu_{k+1}}[r_k + \gamma \nu_{k+1}] = \mathbb{E}_{r_k}[r_k] + \gamma \mathbb{E}_{\nu_{k+1}}[\nu_{k+1}], \quad \mathbb{E}_{\nu_T}[\nu_T] = \mathbb{E}_{v_T}[v_T], \quad (8)$$

$$\mathbb{V}_{\nu_k}[\nu_k] = \mathbb{V}_{r_k \nu_{k+1}}[r_k + \gamma \nu_{k+1}] = \mathbb{V}_{r_k}[r_k] + \gamma^2 \mathbb{V}_{\nu_{k+1}}[\nu_{k+1}], \quad \mathbb{V}_{\nu_T}[\nu_T] = \mathbb{V}_{v_T}[v_T]. \quad (9)$$

We can therefore compute the variance $\mathbb{V}_\nu[\nu_0|o_t, a_{0:T-1}]$ using one forward pass through the selected path computing all \bar{s}_k and $\bar{\Sigma}_k$, starting with the observation encoding $\bar{s}_0 = g(o_t)$, and one backwards pass computing $\mathbb{E}_{\nu_k}[\nu_k]$ and $\mathbb{V}_{\nu_k}[\nu_k]$.

As stated, the above derivation applies to any type of uncertainty that is encapsulated in the distribution that is propagated. For the purpose of driving exploration using uncertainty from sources that are epistemic, we employ epistemic uncertainty estimators such as deep ensembles to estimate the (co-)variances $\Sigma(s_k, a_k), \sigma_r^2(s_k, a_k), \sigma_v^2(s_T)$. To avoid modifying MuZero’s planning further and allow for this approach to remain modular from the specific algorithm it is incorporated into, we interpret MuZero’s representation g , dynamics f , value v and reward r functions as outputting the conditional means $\hat{s}_0 := \hat{s}_0, \hat{s}_k := \hat{s}_k, \hat{v}_T := \hat{v}_T, \hat{r}_k := \hat{r}_k$, respectively.

3.2 PLANNING FOR EXPLORATION

The UCT operator of MCTS takes into account uncertainty *sourced in the planning tree* in the form of a node visitation count (equation 1), to drive exploration *inside* the planning tree. To drive exploration in the environment, we add the environmental epistemic uncertainty into the UCT in a similar manner, as the averaged standard deviation:

$$a_{k-1} := \arg \max_a q(n_{k-1}, a) + 2C_p \sqrt{\frac{2 \log(\sum_{a'} N(n_{k-1}, a'))}{N(n_{k-1}, a)}} + C_\sigma \sqrt{\frac{\sigma_\nu^2}{N(n_{k-1}, a)}}. \quad (10)$$

$C_\sigma \geq 0$ is a constant that can be tuned per task to encourage more or less exploration. The term $\sigma_\nu^2 = \sum_{i=1}^{N(n_{k-1}, a)} \mathbb{V}_{\nu_k^i}[\nu_k^i]$ sums the variances computed individually at every backup step i through node n_k . At each backup step i , with actions a_k^i , state means \bar{s}_k^i and covariances $\bar{\Sigma}_k^i$, the variance $\mathbb{V}_{\nu_k^i}[\nu_k^i]$ is approximated based on equations 9 and 6:

$$\mathbb{V}_{\nu_k^i}[\nu_k^i] \approx \sigma_r^2(\bar{s}_k^i, a_k^i) + \mathbf{J}_r(\bar{s}_k^i, a_k^i) \bar{\Sigma}_k^i \mathbf{J}_r(\bar{s}_k^i, a_k^i)^\top + \gamma^2 \mathbb{V}_{\nu_{k+1}^i}[\nu_{k+1}^i]. \quad (11)$$

$\mathbb{V}_{\nu_{k+1}^i}[\nu_{k+1}^i]$ is computed iteratively backwards during the backup, starting from the last node to be expanded $k = T$, where equation 7 is used:

$$\mathbb{V}_{\nu_T^i}[\nu_T^i] \approx \sigma_v^2(\bar{s}_T^i) + \mathbf{J}_v(\bar{s}_T^i) \bar{\Sigma}_T^i \mathbf{J}_v(\bar{s}_T^i)^\top. \quad (12)$$

Approaches to incorporating OP2E into other search heuristics such as PUCT (which is used by MuZero) can be found in appendix B.1. Action selection in the environment can be done in the same manner as for exploitation (for example, sampling actions with respect to the visitation counts of each action at the root of the tree, in the original MuZero), but based on the exploratory tree.

3.3 LEARNING FROM EXPLORATORY DECISIONS

If the policy executed in the environment is exploratory, in particular with deep exploration that is consistent over multiple time-steps, the targets generated by a somewhat on-policy algorithm such as MuZero (see section 2.3) will reflect an exploratory policy and not the exploitation policy the agent is expected to learn. To alleviate this, we propose three main modifications to the training process which build off of each other: 1) separating training into alternating *exploration/exploitation episodes*, 2) *double planning* and 3) *max targets*. The extensions we propose enable generating value targets that are off-policy both online as well as during Reanalyses. In addition, we maintain some targets that are on-policy but yield better observed returns. These extensions are natural to combine with Reanalyse for further stabilizing of learning from exploratory trajectories.

Alternating episodes First, we propose to alternate between two types of training episodes: *exploratory* episodes that follow an exploration policy throughout the episode, and *exploitatory* episodes that follow a reward-maximizing exploitation policy throughout the episode. This enables us to provide the agent with quality exploitation targets to evaluate and train the value and policy functions reliably, while also providing a large amount of exploratory samples, that explore the environment much more effectively and are more likely to encounter high-reward interactions earlier in the agent’s training. In our experiments we used a ratio of one exploration episode per one exploitation episode, but other ratios as well as dynamically changing ratios are also natural to use. We leave an investigation into optimal exploration / exploitation ratios to future work.

Double planning Second, we propose to compute two separate planning trees at each time step in exploration episodes: an exploration tree following the heuristic in Equation 10 and an exploitation tree following the regular UCT heuristic in Equation 1. When generating value targets from exploration trajectories, the value bootstrap v_{t+n}^π used in the target is the value approximated by the tree planning with exploitation policy $\pi = \pi_\rho$ instead of tree planning with an exploration policy $\pi = \pi_\sigma$:

$$v_t^{target} = \sum_{i=0}^{n-1} \gamma^i r_{t+i}^{\pi_\sigma} + \gamma^n v_{t+n}^{\pi_\rho}. \quad (13)$$

This enables generating off-policy value-bootstraps $v_{t+n}^{\pi_\rho}$ online (similar to Reanalyse’s process offline), but it’s important to note that the rewards $\sum_{i=t}^{n-1} \gamma^i r_{t+i}^{\pi_\sigma}$ in the n-step value target are still the rewards observed in the environment following the exploration policy π_σ . While this doubles the computation cost of planning (or halves the computation budget for each planning tree), the results presented by Danihelka et al. (2021) showed that with a modified version of MuZero the contribution of a large planning budget reduces significantly, and with it, the expected consequence of halving it.

Max targets Third, when generating value targets from exploration episodes, we propose to evaluate whether the exploratory interactions resulted in an improved return compared to the approximation of the MCTS (a *positive* exploration trajectory, left) or not (a *negative* exploration trajectory, right):

$$\sum_{i=t}^{n-1} \gamma^i r_{t+i}^{\pi_\sigma} + \gamma^n v_{t+n}^{\pi_\rho} > v_t^{\pi_\rho}, \quad \sum_{i=t}^{n-1} \gamma^i r_{t+i}^{\pi_\sigma} + \gamma^n v_{t+n}^{\pi_\rho} \leq v_t^{\pi_\rho}. \quad (14)$$

In positive exploration trajectories, the n-step exploratory value target $v_t^{n-step} = \sum_{i=t}^{n-1} \gamma^i r_{t+i}^{\pi_\sigma} + \gamma^n v_{t+n}^{\pi_\rho}$ can be used. In negative exploration trajectories, a zero-step exploitatory target can be used

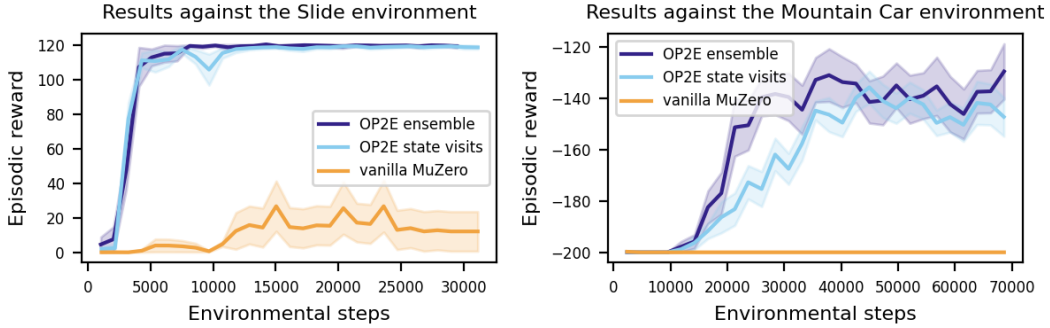


Figure 1: vanilla MuZero vs. OP2E with ensemble-variance uncertainty vs. OP2E with state-visitation-counting uncertainty against both environments. The performance of 10 independent seeds is averaged, and standard error of the mean (SEM) is presented in the shaded area. Both variants of OP2E are able to solve both tasks effectively while vanilla MuZero is not able to solve either of the tasks at all, on average, under the training-steps budget.

instead $v^{0\text{-step}} = v_t^{\pi^{\rho}}$. This is equivalent to generating the value targets with a max operator:

$$v_t^{\text{target}} = \max(v_t^{n\text{-step}}, v_t^{0\text{-step}}). \quad (15)$$

Similarly, policy targets for exploratory episodes can be generated based on a max operator in a similar manner, where the policy used as the target is the policy that has achieved the largest value:

$$\pi^{\text{target}} = \arg \max_{\pi} (v_t^{n\text{-step}}, v_t^{0\text{-step}}). \quad (16)$$

While this enables us to generate off-policy targets from negative exploration trajectories, the presence of 0-step value targets may cause other effects that are detrimental to learning. We explore some of the effects of this series of modifications in an ablation study in the experiments section. In addition, we note that the *max targets* approach only applies to environments with deterministic reward schemes.

4 EXPERIMENTS

To evaluate OP2E we compare the modified exploratory MuZero to vanilla MuZero against two hard-exploration tasks: Slide, a toy task similar to the Chain environment (Osband et al., 2016) to evaluate the extent to which deep exploration is achieved, as well as Mountain Car (Moore, 1990) which is a standard hard-exploration task used to evaluate advanced exploration approaches. In Slide, the environment consists of a chain of 50 states, with the only positive reward at the rightmost end of the chain and 0 rewards otherwise. The agent has access to three actions: left, right, stay. Left results in sliding back 10 positions, or otherwise to the starting position. Right results in proceeding to the right by 1 position. Stay results in sliding back 5 positions. This results in an environment that is very adversarial to exploration that relies on random action selection. In both tasks two variants of OP2E are evaluated: one with deep ensembles with prior functions (*OP2E ensemble*) for a scalable, realistic uncertainty estimation mechanism, and one with discretized state visitation counting (*OP2E state visits*) as an example of a reliable but unrealistic epistemic uncertainty estimation. As a proof of concept, and to avoid modifying MuZero more than absolutely necessary, we replace the state-uncertainty covariance function $\Sigma(s, a)$ with 0, i.e. ignored uncertainty of the forward model.

With the exception of the exploration coefficient C_{σ} (see appendix B.5) no dedicated tuning of hyperparameters was conducted for any of the variations or tasks used in the experiments. The results against both tasks are presented in Figure 1. OP2E is able to effectively solve both tasks, while vanilla MuZero is unable to solve the tasks at all under the training-steps budget provided.

4.1 ABLATIONS

An ablation study of the different modifications proposed for learning from exploratory trajectories in the Mountaincar environment are presented in Figure 2. The state-visitation counting uncertainty

estimator (exploratory state visits) was used in all ablation experiments. In all ablations, the *max targets* agent is an agent with all modifications to training and target generation introduced in Section 3.3 applied: max value targets (eq. 15), max policy targets (eq. 16), alternating between exploration and exploitation episodes and double planning. In every ablation study only one modification is investigated and all other modifications are left active. For example, in the *value targets ablation study* (top left of Figure 2) the value targets are varied, and in the *policy targets ablation study* (top right of Figure 2) the policy targets are varied, but all other design decisions remain the same as in Figure 1. *Value targets ablations* compare between four variants of value targets: max targets, n-step targets, 0-step targets in exploration episodes, and 0-step targets in all (both exploratory and exploitative) episodes. *Policy target ablations* compare between three variants of policy targets: max targets, only-exploratory policy targets (policy targets in exploratory episodes are generated by the exploratory planning trees) and only-exploitative policy targets (policy targets are generated from exploitative planning trees in all episodes). *Alternating episodes ablations* compare between four variants: max value targets with alternating episodes, max value targets without alternating episodes (all episodes are exploration episodes), n-step value targets with alternating episodes, n-step value targets without alternating episodes (all episodes are exploration episodes). Finally, *double planning ablations* compares between an agent that uses double planning and an agent that does not (all episodes are exploratory, all value bootstraps and policy targets are exploratory).

In all experiments in the ablation study the *max targets* variant which uses all modifications proposed in section 3.3 dominates or matches the performance of all other variants in terms of final policy as well as learning stability.

While relying on 0-step value targets to turn MuZero into a completely off-policy algorithm is clearly not a conducive approach, Using max value targets demonstrates an ability to overcome this effect (Figure 2, top left). Generating policy targets based on exploitative trees even in exploration episodes shows significant slowdown of learning (Figure 2, top right). This implies that using Reanalyse to update policy targets from exploratory trajectories with exploitative policy targets, without utilizing the max operator to discern between positive and negative exploration trajectories, can slow down learning significantly. We expect such a slowdown to occur as a result of diverting the agent away from high return exploratory trajectories that differ significantly from the agent’s current exploitation policy. Alternating between exploration and exploitation episodes showed significant slowing of learning to reach the goal state, while showing slightly better final policy and learning stability (Figure 2, bottom left). We expect the delay in learning to be a result of alternating episodes with a ratio of 1 to 1, and better ratios to be able to provide the same benefit with less drawback.

5 RELATED WORK

Plan2Explore (P2E, Sekar et al., 2020) is a previous approach that harnesses planning with learned models and uncertainty for advanced exploration, although in a different setting to the one tackled in this paper. P2E proposes pre-training of an exploration policy for a task, without access to a reward signal. The policy is trained to choose actions that maximize the epistemic uncertainty associated with the transition model. This policy is regularly updated with newly collected samples, until the entire state space is sufficiently explored and the learned model therefore precise enough everywhere to plan well. P2E only considers state prediction uncertainty and propagates the uncertainty through planning as intrinsic reward as opposed to variance. In addition, P2E requires an extended pre-training phase and does not scale to large state-spaces, because the learned exploration policy is trained to explore the entire state space without trading off for more promising areas with respect to expected return. In contrast, our approach propagates the uncertainty explicitly, enables a trade-off in real time between exploration and exploitation and is applicable to the standard online exploration setting in RL.

Epistemic uncertainty has developed into a standard for driving exploration in RL with methods such as Bootstrapped-DQN (Osband et al., 2016), the uncertainty Bellman-equation (UBE, O’Donoghue et al., 2018) and intrinsic reward (IR, Oudeyer & Kaplan, 2009). UBE approximates an analytically-motivated upper bound on the epistemic uncertainty associated with Q-values, in the form of a variance. The variance is used to drive exploration using Thompson sampling. UBE has not been developed explicitly for model-based approaches, and thus does not consider transition-based uncertainty, nor does it take advantage of the ability of online planning to propagate information from

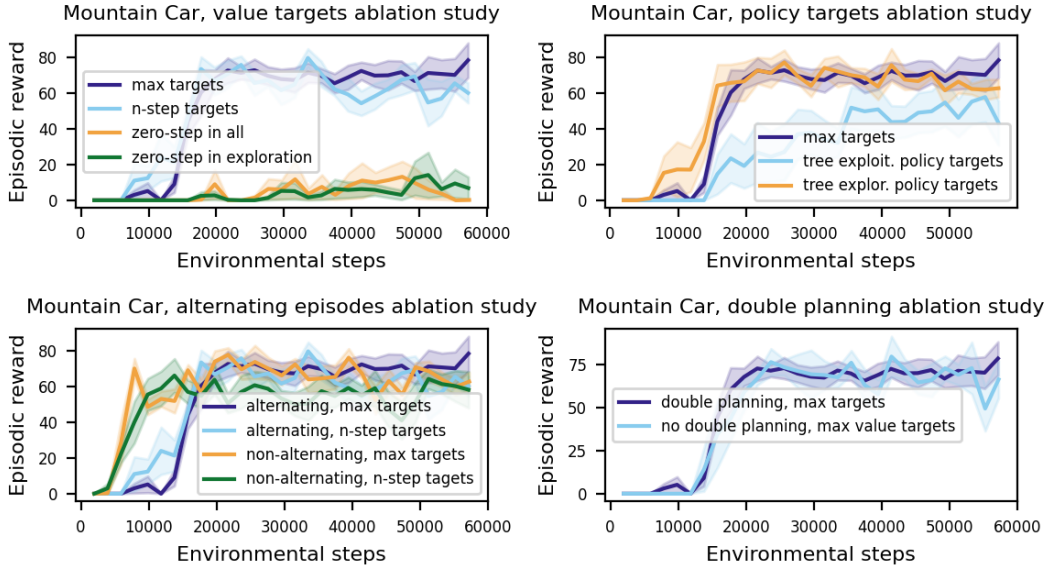


Figure 2: Target ablations against Mountain Car. The performance of 5 independent seeds is averaged, and standard error of the mean (SEM) is presented in the shaded area. A modified reward scheme is used for Mountain Car, see appendix B.4 for details.

future decisions into current decisions immediately. In IR the epistemic uncertainty propagates directly through the learned Q-value function, by learning a modified function:

$$Q_{IR}^{\pi}(s_t, a_t) = \mathbb{E}[r(s_t, a_t) + u(s_t, a_t) + \gamma V^{\pi}(s_{t+1}) | s_{t+1} \sim P(\cdot | s_t, a_t)]$$

Where $u(s_t, a)$ is an uncertainty-bonus that is used to encourage the agent to explore less-visited transitions. Coupled with the limitations, a strength of propagating the uncertainty through value learning compared to through planning is that the horizon of uncertainty propagation is not limited to the horizon of the planning (which is logarithmic in the planning budget of a planning tree in the worst case, and linear in the best case). Instead, the horizon is limited by the number of learning steps, which constrains the propagation differently. For example, deep Q-networks (DQN, Mnih et al., 2015) make one gradient update-step per environmental step, whereas planning always propagates immediately until the planning horizon. Moreover, these methods can be combined with our approach by using UBE to replace uncertainty-in-leaf value prediction in MuZero. Propagating newly discovered uncertainty until the planning horizon happens immediately with our method, whereas longer delays are propagated through the value function.

6 CONCLUSIONS

Propagating epistemic uncertainty in real time with a planning tree and modifying the planning objective to an exploratory objective have together demonstrated effective deep exploration, while circumventing common issues arising from propagating uncertainty through value learning. In addition, the extensions we propose to learning from consistently-exploratory decisions show capacity to reach better final policies in addition to a more stable learning process, effects which we expect to grow stronger in the presence of environments with more complex reward schemes and a more varied range of near-optimal policies. The framework developed for approximating the epistemic uncertainty as it propagates in a planning tree can provide a backbone for additional approaches that take advantage of uncertainty estimation, such as planning for reliable execution (by discouraging uncertain decisions) or reliable planning (by avoiding planning into trajectories where additional planning *increases* uncertainty). The propagation framework itself is essentially modular from both MuZero and MCTS, making it an available choice for any approach that plans with a learned model and planning trees. Our approach strengthens the notion that incorporating epistemic uncertainty into different online inference mechanisms has the potential to provide effective exploration by harnessing the strengths of the mechanism to make better exploratory decisions.

ACKNOWLEDGMENTS

We would like to thank Marco Loog, Frank van der Meulen, Moritz Zanger, Pascal van der Vaart & Joery de Vries for creative discussions and fruitful feedback.

REFERENCES

- Karl Johan Åström. Optimal control of markov processes with incomplete state information i. *Journal of Mathematical Analysis and Applications*, 10:174–205, 1965.
- Marc Bellemare, Sriram Srinivasan, Georg Ostrovski, Tom Schaul, David Saxton, and Remi Munos. Unifying count-based exploration and intrinsic motivation. *Advances in neural information processing systems*, 29, 2016.
- Richard Bellman. A markovian decision process. *Journal of mathematics and mechanics*, 6(5):679–684, 1957.
- Cameron B Browne, Edward Powley, Daniel Whitehouse, Simon M Lucas, Peter I Cowling, Philipp Bohnhorst, Stephen Tavener, Diego Perez, Spyridon Samothrakis, and Simon Colton. A survey of monte carlo tree search methods. *IEEE Transactions on Computational Intelligence and AI in games*, 4(1):1–43, 2012.
- Ivo Danihelka, Arthur Guez, Julian Schrittwieser, and David Silver. Policy improvement by planning with gumbel. In *International Conference on Learning Representations*, 2021.
- Joery de Vries, Ken Voskuil, and Frank Bryce. Muzero. *GitHub repository*, 2021. <https://github.com/kaesve/muzero/tree/ee990aa4927a6ec34eef6928da50446b40f3685f>.
- Werner Duvaud. muzero-general. *GitHub repository*, 2021. <https://github.com/werner-duvaud/muzero-general/tree/23a1f6910e97d78475ccd29576cdd107c5afefd2>.
- Jean-Bastien Grill, Florent Alché, Yunhao Tang, Thomas Hubert, Michal Valko, Ioannis Antonoglou, and Rémi Munos. Monte-carlo tree search as regularized policy optimization. In *International Conference on Machine Learning*, pp. 3769–3778. PMLR, 2020.
- Johanna Hansen. bootstrap_dqn. *GitHub repository*, 2019. https://github.com/johannah/bootstrap_dqn/tree/734fd78a776cc940da40d5ce5f3775b5ce7cac7d.
- Eyke Hüllermeier and Willem Waegeman. Aleatoric and epistemic uncertainty in machine learning: An introduction to concepts and methods. *Machine Learning*, 110(3):457–506, 2021.
- Moksh Jain, Salem Lahlou, Hadi Nekoei, Victor Butoi, Paul Bertin, Jarrid Rector-Brooks, Maksym Korablyov, and Yoshua Bengio. Deup: Direct epistemic uncertainty prediction. *arXiv preprint arXiv:2102.08501*, 2021.
- Levente Kocsis and Csaba Szepesvári. Bandit based monte-carlo planning. In *European conference on machine learning*, pp. 282–293. Springer, 2006.
- Amol Mandhane, Anton Zhernov, Maribeth Rauh, Chenjie Gu, Miaosen Wang, Flora Xue, Wendy Shang, Derek Pang, Rene Claus, Ching-Han Chiang, et al. Muzero with self-competition for rate control in vp9 video compression. *arXiv e-prints*, pp. arXiv–2202, 2022.
- Volodymyr Mnih, Koray Kavukcuoglu, David Silver, Andrei A Rusu, Joel Veness, Marc G Bellemare, Alex Graves, Martin Riedmiller, Andreas K Fidjeland, Georg Ostrovski, et al. Human-level control through deep reinforcement learning. *nature*, 518(7540):529–533, 2015.
- Andrew William Moore. Efficient memory-based learning for robot control. Technical report, University of Cambridge, 1990.

- Frank Nielsen. On the jensen-shannon symmetrization of distances relying on abstract means. *Entropy*, 21(5), 2019. ISSN 1099-4300. doi: 10.3390/e21050485. URL <https://www.mdpi.com/1099-4300/21/5/485>.
- Brendan O’Donoghue, Ian Osband, Remi Munos, and Volodymyr Mnih. The uncertainty bellman equation and exploration. In *International Conference on Machine Learning*, pp. 3836–3845, 2018.
- Ian Osband, Charles Blundell, Alexander Pritzel, and Benjamin Van Roy. Deep exploration via bootstrapped dqn. *Advances in neural information processing systems*, 29:4026–4034, 2016.
- Ian Osband, John Aslanides, and Albin Cassirer. Randomized prior functions for deep reinforcement learning. *arXiv preprint arXiv:1806.03335*, 2018.
- Pierre-Yves Oudeyer and Frederic Kaplan. What is intrinsic motivation? a typology of computational approaches. *Frontiers in neurorobotics*, 1:6, 2009.
- Daniel J Russo, Benjamin Van Roy, Abbas Kazerouni, Ian Osband, Zheng Wen, et al. A tutorial on thompson sampling. *Foundations and Trends® in Machine Learning*, 11(1):1–96, 2018.
- Julian Schrittwieser, Ioannis Antonoglou, Thomas Hubert, Karen Simonyan, Laurent Sifre, Simon Schmitt, Arthur Guez, Edward Lockhart, Demis Hassabis, Thore Graepel, et al. Mastering atari, go, chess and shogi by planning with a learned model. *Nature*, 588(7839):604–609, 2020.
- Julian Schrittwieser, Thomas Hubert, Amol Mandhane, Mohammadamin Barekatain, Ioannis Antonoglou, and David Silver. Online and offline reinforcement learning by planning with a learned model. *Advances in Neural Information Processing Systems*, 34:27580–27591, 2021.
- Ramanan Sekar, Oleh Rybkin, Kostas Daniilidis, Pieter Abbeel, Danijar Hafner, and Deepak Pathak. Planning to explore via self-supervised world models. In *International Conference on Machine Learning*, pp. 8583–8592. PMLR, 2020.
- David Silver, Aja Huang, Chris J Maddison, Arthur Guez, Laurent Sifre, George Van Den Driessche, Julian Schrittwieser, Ioannis Antonoglou, Veda Panneershelvam, Marc Lanctot, et al. Mastering the game of go with deep neural networks and tree search. *nature*, 529(7587):484–489, 2016.
- David Silver, Julian Schrittwieser, Karen Simonyan, Ioannis Antonoglou, Aja Huang, Arthur Guez, Thomas Hubert, Lucas Baker, Matthew Lai, Adrian Bolton, et al. Mastering the game of go without human knowledge. *nature*, 550(7676):354–359, 2017.
- David Silver, Thomas Hubert, Julian Schrittwieser, Ioannis Antonoglou, Matthew Lai, Arthur Guez, Marc Lanctot, Laurent Sifre, Dharshan Kumaran, Thore Graepel, et al. A general reinforcement learning algorithm that masters chess, shogi, and go through self-play. *Science*, 362(6419):1140–1144, 2018.

A LAW OF TOTAL VARIANCE

The *law of total variance* for two continuous random variables X and Y can be derived as follows:

$$\begin{aligned}
 \mathbb{V}_Y[Y] &= \int (Y - \mathbb{E}_Y[Y])^2 p(Y) dY = \iint (Y - \mathbb{E}_Y[Y])^2 p(X, Y) dX dY \\
 &= \iint (Y - \mathbb{E}_Y[Y])^2 p(Y|X) p(X) dX dY = \mathbb{E}_X \left[\mathbb{E}_Y \left[(Y - \mathbb{E}_Y[Y])^2 | X \right] \right] \\
 &= \mathbb{E}_X \left[\mathbb{E}_Y \left[(Y - \mathbb{E}_Y[Y|X] + \mathbb{E}_Y[Y|X] - \mathbb{E}_Y[Y])^2 | X \right] \right] \\
 &= \mathbb{E}_X \left[\underbrace{\mathbb{E}_Y \left[(Y - \mathbb{E}_Y[Y|X])^2 | X \right]}_{\mathbb{V}_Y[Y|X]} + 2 \underbrace{\mathbb{E}_Y \left[(Y - \mathbb{E}_Y[Y|X]) (\mathbb{E}_Y[Y|X] - \mathbb{E}_Y[Y]) \right]}_0 \right] \\
 &\quad + \underbrace{\mathbb{E}_X \left[(\mathbb{E}_Y[Y|X] - \mathbb{E}_Y[Y])^2 \right]}_{\mathbb{V}_X[\mathbb{E}_Y[Y|X]]} = \mathbb{V}_X[\mathbb{E}_Y[Y|X]] + \mathbb{E}_X[\mathbb{V}_Y[Y|X]]
 \end{aligned}$$

B EXPERIMENTAL SETUP

This section contains additional information regarding the choices of epistemic uncertainty estimation in the functions used by MuZero, modifications to the reward scheme of the environments used in the evaluation, and specific hyper parameter choices and tuning.

B.1 OP2E WITH OTHER MCTS SEARCH HEURISTICS

The UCT search heuristic is not the heuristic used by MuZero. Instead, MuZero uses a variant called probabilistic upper confidence tree (PUCT) bound (see MuZero’s appendices at (Schrittwieser et al., 2020)):

$$a_k = \arg \max_{a \in A} q(\hat{s}_k, a) + \pi(\hat{s}_k, a) \lambda_{\hat{s}_k, a}, \quad (17)$$

where $\lambda_{\hat{s}_k, a} = \frac{\sqrt{\sum_{a'} N(\hat{s}_k, a')}}{1 + N(\hat{s}_k, a)} \left[C_1 + \log \left(\frac{N(\hat{s}_k, a') + C_2 + 1}{C_2} \right) \right]$ and where $\pi(\hat{s}_k, a)$ is the probability of taking action a at node \hat{s}_k according to the policy network π . A key difference between the two heuristics is that PUCT takes into account some prior knowledge over the outcomes of the actions in terms of $\pi(\hat{s}_k, a)$, while UCT does not involve a prior policy. In addition, since the publication of MuZero other search criteria have been proposed, such as the precise solution to the regularized policy optimization problem (Grill et al., 2020) and a variation of this approach by (Danihelka et al., 2021).

To incorporate OP2E into PUCT, in our experiments we have modified PUCT similarly to the proposed modification to UCT, by adding the environmental uncertainty in the value prediction as an additional term, in the form of the average standard deviation:

$$a_{k-1} = \arg \max_{a \in A} q(\hat{s}_{k-1}, a) + \pi(\hat{s}_{k-1}, a) \lambda_{\hat{s}_{k-1}, a} + C_\sigma \sqrt{\frac{\sigma_v^2}{N(\hat{s}_{k-1}, a)}}. \quad (18)$$

Incorporating OP2E into the criteria used by the more recent approaches can be done by treating the averaged standard deviation term $C_\sigma \sqrt{\frac{\sigma_v^2}{N(\hat{s}_{k-1}, a)}}$ as directly part of the Q-value and replacing every estimate of $q(\hat{s}_{k-1}, a)$ with $q(\hat{s}_{k-1}, a) + C_\sigma \sqrt{\frac{\sigma_v^2}{N(\hat{s}_{k-1}, a)}}$. Deciding whether these modification should be extended to the policy targets generated based on these estimates can follow the reasoning of max policy targets from section 3.3.

B.2 ESTIMATING EPISTEMIC VALUE AND REWARD UNCERTAINTY WITH STATE VISITATION COUNTING

Counting of state-action pairs’ visitations can naturally be used as an epistemic uncertainty estimate. We identify three challenges to incorporating this epistemic uncertainty estimator into MuZero: 1) MuZero is planning with *abstracted* states, while the counter is designed to work against discrete real states of the system. 2) Our method requires (at least) two independent estimates for the uncertainty: one in reward, and one in value, while state visitation counting provides a single source for uncertainty estimation. 3) Estimating uncertainty in continuous state-space environments, such as Mountain Car. In this section, we will describe the approaches used to overcome each one of those challenges.

B.2.1 ESTIMATING COUNTING UNCERTAINTY IN PLANNING

In order to estimate the uncertainty associated with *real* states during planning, we allow MuZero access to a real model of the environment. This of course violates the assumption that MuZero is able to learn entirely from interactions with the environment without access to any prior knowledge. This is only introduced in order to evaluate the soundness of our method, and the real model is only used to estimate the uncertainty with planned actions. The second uncertainty estimation method we use, ensembles, does not violate any such assumptions. The epistemic uncertainty in reward-prediction is estimated as follows:

$$u_{r_k} = \beta \frac{1}{n_{s_k} + \epsilon}$$

Where n_{s_k} denotes the count of visitations to *real* state s_k , the state associated with action trajectory $a_{0:k}$ and observation o in a deterministic environment. β is some constant used to scale the uncertainty, and ϵ is a constant used to guarantee numerical stability when $n_{s_k} = 0$. During the MCTS planning phase, in each expansion step, the agent uses the real model to predict the transition associated with the chosen action from the chosen state, and uses this prediction to estimate the reward uncertainty.

B.2.2 CREATING SEPARATE ESTIMATES FOR REWARD UNCERTAINTY AND VALUE UNCERTAINTY

In order to use state visitation counting as an independent uncertainty estimate for both the value of a *leaf* planning-tree-node k as well as the reward predicted for a transition k , we employ two ideas: 1) we assume that the reward uncertainty of future transitions $u_{r_{k+i}}, \forall i > 0$, can be crudely estimated as equal the local reward uncertainty u_{r_k} without completely debilitating the value uncertainty estimation’s reliability. 2) We utilize a similar approach to MC simulations to arrive at an approximation of the value uncertainty u_{v_k} that is expected to be better than that provided by 1).

We combine both ideas to arrive at a final computation for the value-uncertainty estimate for leaf-node k . First, the agent plans from real state s_k forward, using the real model, with some action-selection policy π_σ one trajectory h steps into the future. At each step, the agent evaluates the uncertainty of each transition with the state-counter. Second, upon arriving at step $k+h$, the agent uses the geometric-series formula to approximate the uncertainty of following the same policy to infinity, with the approximation that all uncertainties from state s_{k+h} into the future, following policy π_σ , are constant and equal $u_{r_{k+h}}$:

$$u_{v_k} \approx \sum_{i=0}^{h-1} \gamma^{2i} u_{r_{k+i}} + \gamma^{2h} u_{v_{k+h}} \approx \sum_{i=0}^{h-1} \gamma^{2i} u_{r_{k+i}} + \sum_{i=h}^{\infty} \gamma^{2i} u_{r_{k+h}} = \sum_{i=0}^{h-1} \gamma^{2i} u_{r_{k+i}} + \frac{\gamma^{2h}}{1-\gamma^2} u_{r_{k+h}}$$

The first step approximates u_{v_k} as the discounted sum of reward-uncertainties along the trajectory $a_{k:k+h-1}$, and then with an as yet unknown discounted end-of-trajectory value-uncertainty estimate $u_{v_{k+h}}$. The second step approximates the end-of-trajectory value-uncertainty estimate $u_{v_{k+h}}$ as the sum of a geometric series with the constant reward uncertainty attained at the end of the trajectory, $u_{r_{k+h}}$. The policy π_σ we chose to follow is "repeat action a_{k-1} ". For example, if the action leading to planning node k was "accelerate to the right", π_σ chooses "accelerate to the right" for all actions along the trajectory $a_{k:k+h}$. This enables u_{v_k} to propagate information from future decisions that (may) be taken by the algorithm, which should provide rather-independent uncertainty estimation from the local reward uncertainty estimates u_{r_k} .

B.2.3 EXTENDING STATE- VISITATIONS COUNTING TO CONTINUOUS STATE-SPACE ENVIRONMENTS

The state space of the Mountain Car environment is continuous. In order to employ visitations-counting in a continuous position-velocity state-space environment, we use discretization of the state-space to a 50 by 50 grid of possible position-velocity combinations, which is made possible because the ranges of both the velocity as well as the positions are finite.

B.3 ESTIMATING EPISTEMIC VALUE AND REWARD UNCERTAINTY WITH AN ENSEMBLE

Estimating the same quantities with the ensemble is done in a much more straight forward manner. The variance in the predictions of the different ensemble members is computed, and is used as the direct measure of the uncertainty in each function - reward and value. MuZero predicts the rewards and values using a categorical representation rather than a simple regression to scalar, however. The categorical representation can represent numbers in the range $(-support, support)$, for some hyperparameter *support* that specifies the size of the output layer of the network, which is $support \times 2 + 1$. The vector-output of the network is passed through a SoftMax function. The weights of the categorical distribution are multiplied by the values represented by the $(-support, support)$. Finally, the entries are summed to produce the final prediction. This architecture introduces an additional challenge to the variance computation - rather than computing the variance over a set of scalars, now one is presented with a set of distributions over which to compute the variance.

As an additional effect of this architecture, we have observed that in under-trained areas of the input space, the networks have tendency to converge to outputs close to 0. We explain this with the claim that for inputs that for the network are arbitrary, the network is likely to produce outputs that are arbitrary. Under the assumption that each entry in the soft-max output vector is somewhat independent from any other for arbitrary inputs, we expect arbitrary outputs for a categorical representation to, on average, not be concentrated in one extreme side of the representation. Further, they are likely to be about as concentrated on one "side" of the vector as on the other, which will reduce the total absolute value of the scalar represented by the vector, pushing it closer to 0. This suspected phenomenon has two noteworthy effects: 1) the variance in the scalar-representation of the ensemble prediction reduces to zero in under-trained areas of the input space, which is exactly adverse to the behavior we require. 2) This results in an implicit, if unreliable, optimistic or pessimistic initialization of rewards and value predictions (depending on the reward scheme of the environment). Specifically, in environments where the true values are all negative and represented by the extreme state of the soft max vector –*support*, this may induce an inherent optimistic-initialization effect to the agent’s value and reward estimates, implicitly encouraging the agent to explore the unknown, because unknown state are associated with value and reward predictions that are more likely to be close to zero. This effect is expected to be even stronger when an ensemble is used, because the averaging effect goes stronger with the size of the ensemble.

In order to mitigate these unintended effects, we have taken two steps. First, we have modified the reward schemes of the environments we have tested against to only produce positive rewards, and only in the goal state, to disable the effect of any unintended optimistic initialization, which may conflict with the method of this work and give the vanilla version an unintended advantage. Second, rather than compute the straight-forward variance in an ensemble as the variance over the translated-to-scalar predictions, we compute the variance as the variance between the entries of the different categorical representation-entries, entry by entry, and sum them as the final variance measure:

$$\mathbb{V}[y] \approx \sum_{i=0}^{2 \times \text{support} + 1} \mathbb{V}[y_i]$$

for $y \in [0, 1]^{2 \times \text{support} + 1}$ denoting the categorical-vector output of the NN. An additional variance computation that was considered but had not shown advantage in our preliminary experiments was computing the average categorical distribution of the ensemble, and then taking the average Jensen-Shannon distance (Nielsen, 2019) between each ensemble-member’s categorical distribution, and the mean categorical distribution. While both approaches cannot be expected to be in the correct scale of the real variance of the scalar reward or value predictions, our experiments show that the entry-by-entry variance, at least, is sufficient to achieve both directed as well as deep exploration (figure 1). In addition, the tuning of the C_σ parameter can alleviate errors in the scale of the variance with respect to the actual rewards and values.

B.4 REWARD SCHEMES

The standard reward scheme of the Mountain Car environment produces a reward of -1 at each time step. The only escape available to the agent is the goal state, which is terminal. The optimal policy induced by this reward scheme is "arrive at the goal in the smallest number of timesteps possible". As mentioned in section B.3, reward schemes that induce negative values are likely to cause unexpected and adverse effects for the purpose of evaluating the modifications to the agent. For this reason, we use an additional non-Markovian reward scheme.

In the non-Markovian reward scheme, the agent receives a reward of 0 at each transition except the transitions into the goal, for which it receives a non-constant reward equal $r_{goal} = T_{timeout} - T_{elapsed}$. $T_{timeout}$ denotes the maximum number of timesteps the environment allows for, before sending a timeout signal and terminating the agent. $T_{elapsed}$ is the number of timesteps elapsed in the environment, up until the agent transitioned into the terminal goal state. While this non-Markovian reward induces a non-Markovian environment, the optimal policy remains the same, and so does the learning process of the agent.

In the final experiments conducted, the effects of the original -1 s reward scheme of Mountain Car that were observed in earlier experiments were not observed, and thus we present experiments against the original reward scheme for the main experiments. The ablations were experimented

against the non-Markovian reward scheme, to reduce any additional influencing factors on the ablations.

B.5 HYPERPARAMETER OPTIMIZATION

The purpose of the main evaluation presented in this work is to illustrate the effect of planning to explore compared to the vanilla version of the algorithm. Further, as the two versions of the algorithm are not too different from each other, we expect that the majority of hyperparameter optimization will effect all versions similarly. For this reason, no dedicated tuning of hyperparameters was conducted as part of the experiments conducted in this work. The hyperparameters used were chosen based on existing implementations for other environments in the original code base (Duvaud, 2021). The network architecture used for mountaincar was based on another implementation of MuZero (de Vries et al., 2021) that was evaluated against the Mountain Car environment.

Two hyperparameters are somewhat exempt from this statement, however. The exploration coefficient c_σ introduced with our proposed methodology for planning for exploration was tuned for each task and for each variant. The temperature parameter T was not tuned explicitly, but a different temperature parameter was used between the different variants. Motivation and description of the reasoning behind the optimization process and the process itself are provided in the following sections.

B.5.1 TEMPERATURES

The temperature parameter T is used by MuZero for action sampling in the environment as follows:

$$a_t \sim p(\cdot), \quad p(a_i) = \frac{N^{\frac{1}{T}}(n_0, a_i)}{\sum_{a' \in A} N^{\frac{1}{T}}(n_0, a')} \quad (19)$$

$p(a_i)$ denotes the probability of sampling action a_i according to the temperature and the visitation counts. When the temperature $T \rightarrow 0$, the probability distribution collapses to greedy action selection according to the maximum number of visitations. When the temperature $T \rightarrow \infty$, the distribution becomes uniform. The temperature induces exploration in the environment through random action selection weighted towards "better" actions from an exploitative perspective, according to the estimates of the tree. As the modifications proposed in this work are meant to provide much more informed exploration, the temperatures used were lower than the original configuration used by other implementations. The original range was $1 \rightarrow 0.25$, and the modified range was $0.25 \rightarrow 0.1$. In the experiments, vanilla MuZero was evaluated both with the lower temperatures used by the planning with uncertainty variants (to not introduce any unexpected advantage from the lower temperatures), as well as with higher temperatures pre-configured for other environments in the code base we built upon, to give MuZero a chance with the weighted random action selection used by MuZero for exploration. There was no significant difference between the performance of the different temperatures with vanilla MuZero. The experiments presented are with higher temperatures. Exact hyperparameters are specified in appendix C.3.

B.5.2 TUNING THE EXPLORATION COEFFICIENT C_σ

The exploration coefficient C_σ (see section 3.2) was tuned independently for each uncertainty mechanism used, and again per environment. The tuning aimed to achieve preference by the UCB of unvisited states over everything else, and the goal-reward over anything except unvisited states. The tuning was stopped upon observation that deep exploration was achieved successfully in most seeds. Once tuning was stopped, the experiments were initiated for the chosen number of seeds (10 for the main experiments and 5 for the ablations). The range of C_σ investigated for the state-visitation-counting method was between 0.1 and 100 and was done using rough and then fine grid-search. The range of C_σ investigated for the ensemble-variance method was between 10^1 and 10^8 and was search with a rough and then fine grid search.

C IMPLEMENTATION

The implementation used to evaluate the agent is accessible in {commented for review}. This implementation was built on the implementation by (Duvaud, 2021), which in turn is built on the official pseudocode released in the original MuZero paper (Schrittwieser et al., 2020). The implementation of the ensemble architecture was based on (Hansen, 2019), which is an implementation of the bootstrapped-DQN with randomize prior networks proposed in (Osband et al., 2018). In the following sections, we specify first the details of the network architecture used, and second the hyperparameters used.

C.1 NETWORK ARCHITECTURE

Two network architectures were used in this work to evaluate the *planning for exploration* methodology. These architecture are divided between agents that used ensemble-variance as an uncertainty mechanism, and the agents that didn't. Both architectures use blocks of feed-forward networks for every estimator used by the agent: 1) the representation function $g(o)$. 2) the transition dynamics $f(s, a)$. 3) the reward function $r(s)$. 4) the value function $v(s)$ and 5) the policy function $\pi(s)$.

Representation function block This feed-forward network consisted of an input layer of size 1 (the dimensionality of the observation space), a hidden layer of size 16, and an output layer of size 4.

Transition dynamics function block This feed-forward network consists of an input layer of size 7 (state-abstraction-encoding size of 4, and action space of 3), two hidden layers of size 16, and an output layer of size 4.

Reward & value function blocks These two feed-forward blocks have identical architecture, consisting of an input layer of size 4, two hidden layer of size 16 and an output layer of size $support \cdot 2 + 1$, for a categorical representation of real numbers, as discussed in section B.3. The support size used was 15, for a output-layer size of 31.

Policy function block This feed forward block used an input layer of size 4, two hidden layers of size 16, and an output layer of size 3, the size of the action space.

Ensemble architecture The architecture of networks used by the ensemble-using agents formulated the relevant blocks (reward and value blocks) as ensembles rather than individual blocks. This translates to having 5 (the ensemble size used) independent blocks of reward, and 5 of value. The prediction from the block is taken as the average of the individual blocks' predictions.

C.2 HYPERPARAMETERS CONFIGURATION

We divide the hyperparameters into 3 distinct classes: 1) *planning for exploration* target-adaptation parameters, such as whether to use n-step or 0-step targets. These parameters are described in the experimental setup, section B. 2) Network-architecture details. These parameters are described in a dedicated appendix, C.1. 3) Additional hyperparameters, such as number of training steps, batch size, learning steps decay, etc. These hyperparameters are detailed in this section, in table 1.

We provide a list of comments for additional details regarding some of the hyper-parameters:

1. The number of nodes in each MCTS planning tree. Preliminary results in Mountain Car with planning budget of 50, showed the same behavior as in the results presented in section 4 but with lower stability.
2. A UCT parameter used by MuZero's MCTS variant. For more details, see (Schrittwieser et al., 2020).
3. A UCT parameter used by MuZero's MCTS variant. For more details, see (Schrittwieser et al., 2020).
4. The implementation maintains a ratio of *Training ratio* between the training steps and the environmental steps. A ratio of x represents x training steps for each environment steps. Additional results attained but not presented in the work experimented with up to 300000 steps. The behavior observed was the same as the one showed in the results presented. Observing that the large number of training steps does not appear to be necessary to demonstrate the capacity of our method, and due to compute and time resource limitations, the experiments with the final hyperparameters, presented in section 4, were conducted with a smaller number of timesteps.

	Slide	Slide, abl.	Mountain Car	Mountain Car, abl.	Comment
Num. of stacked obs.	1	1	1	1	-
Discount parameter γ	0.95	0.95	0.997	0.997	-
Planning nodes budget	30	30	200	200	1
Root dirichlet α	0.25	0.25	0.25	0.25	-
Root exploration fraction	0.25	0.25	0.25	0.25	-
UCB's pb-c-base	19652	19652	19652	19652	2
UCB's pb-c-init	1.25	1.25	1.25	1.25	3
Training steps	70000	45000	120000	100000	4
Traning ratio	2.25	2.25	1.75	1.75	
Batch size	128	128	128	128	-
Value-loss weight	1	1	1	1	5
Training hardware	distributed CPUs	distributed CPUs	distributed CPUs	distributed CPUs	-
Learning rate λ	0.02	0.02	0.02	0.02	6
Rate of λ decay	0.9	0.9	0.9	0.9	
Decay steps c_{steps}	500	500	2000	2000	
Replay buffer size	500	500	1000	1000	-
Unroll steps in loss	10	10	10	10	-
n-step target's n	50	50	50	50	-
Prioritized replay	0.5	0.5	0.5	0.5	7
Reanalyze	True	True	True	True	8
Ensemble size	5	-	5	-	-

Table 1: Hyperparameters used in the results presented in section 4

- MuZero enables scaling of the different losses in the loss computation independently.
- The learning rate decay is computed as follows: $\lambda\rho^{n/c_{steps}}$, for n the current training step count.
- The sampling-priorities of trajectories in the replay buffer are computed as the absolute value of the difference between the value and the value target, to the power of this hyperparameter.
- The rudimentary implementation of MuZero-Reanalyze used in this implementation replaces old value estimates from planning trees with new value estimates from the value function directly, rather than from newly computed planning trees.

C.3 TEMPERATURES

Two ranges of temperatures were used in each environment. The regular temperatures were used to evaluate the vanilla agent, while the low temperatures were used to evaluate the exploratory agent. The exact temperature values are specified in table 2. The regular temperatures' values switched at 0.3, and 0.5 of the total training step budget. The low temperatures' values switched at 0.3, 0.5 and 0.75 of the total training step budget.

	Slide	Mountain Car
Regular	1.0, 0.5, 0.25	1, 0.5, 0.25
Low	0.75, 0.25, 0.175, 0.02	0.5, 0.25, 0.175, 0.1

Table 2: Temperature ranges used in this work